



Nitrogen doped germania glasses with enhanced optical and mechanical properties

Storgaard-Larsen, Torben; Poulsen, Christian; Leistiko, Otto

Published in:
Journal of The Electrochemical Society

Link to article, DOI:
[10.1149/1.1837752](https://doi.org/10.1149/1.1837752)

Publication date:
1997

Document Version
Publisher's PDF, also known as Version of record

[Link back to DTU Orbit](#)

Citation (APA):
Storgaard-Larsen, T., Poulsen, C., & Leistiko, O. (1997). Nitrogen doped germania glasses with enhanced optical and mechanical properties. *Journal of The Electrochemical Society*, 144(6), 2137-2142.
<https://doi.org/10.1149/1.1837752>

General rights

Copyright and moral rights for the publications made accessible in the public portal are retained by the authors and/or other copyright owners and it is a condition of accessing publications that users recognise and abide by the legal requirements associated with these rights.

- Users may download and print one copy of any publication from the public portal for the purpose of private study or research.
- You may not further distribute the material or use it for any profit-making activity or commercial gain
- You may freely distribute the URL identifying the publication in the public portal

If you believe that this document breaches copyright please contact us providing details, and we will remove access to the work immediately and investigate your claim.

21. W. Müller-Markgraf and M. J. Rossi, *Rev. Sci. Instrum.*, **61**, 1217 (1990).
22. V. Ilderem and R. Reif, *This Journal*, **135**, 2569 (1988).
23. T. Sunada, T. Yasaka, M. Takakura, T. Sugiyama, S. Miyazaki, and M. Hirose, *Jpn. J. Appl. Phys.*, **29**, L2408 (1990).
24. M. A. Mendicino, Ph.D. Thesis, University of Illinois at Urbana-Champaign (1994).
25. W. K. Chu, H. Kroutle, J. W. Mayer, H. Muller, M. A. Nicolet, and K. N. Tu, *Appl. Phys. Lett.*, **25**, 454 (1974).
26. J. Engqvist, C. Myers, and J.-O. Carlsson, *This Journal*, **139**, 3197 (1992).
27. R. Ditchfield, M. A. Mendicino, and E. G. Seebauer, *ibid.*, **143**, 266 (1996).
28. K. Saito, T. Amazawa, and Y. Arita, *ibid.*, **140**, 513 (1993).
29. D. W. Williams, E. Coleman, and J. M. Brown, in *Proceedings of the Workshop on Tungsten and Refractory Metals for VLSI Applications*, R. S. Blewer, Editor, p. 125, MRS, Pittsburgh, PA (1985).
30. L. A. Clevenger, J. M. E. Harper, C. Cabral, C. Nobili, G. Ottaviani, and R. Mann, *J. Appl. Phys.*, **72**, 4978 (1992).
31. A. Bouteville, A. Royer, and J. C. Remy, *This Journal*, **134**, 2080 (1987).
32. R. P. Southwell and E. G. Seebauer, *J. Vac. Sci. Technol.*, **A13**, 221 (1995).
33. H. de Lanerolle, B. Kim, L. Moser, Y. Zheng, D. Steiner, and J. Berg, *J. Electron. Mater.*, **19**, 1185 (1990).
34. R. P. Southwell and E. G. Seebauer, *Surf. Sci.*, **329**, 187 (1995).
35. Z. Ma, L. H. Allen, and D. D. J. Allman, *J. Appl. Phys.*, **77**, 4384 (1995).
36. M. A. Mendicino and E. G. Seebauer, *Surf. Sci.*, **277**, 89 (1992).
37. S. M. Gates, C. M. Greenlief, D. B. Beach, and P. A. Holbert, *J. Chem. Phys.*, **92**, 344 (1990).
38. M. A. Mendicino and E. G. Seebauer, *This Journal*, **140**, 1786 (1993).
39. S. M. Gates, C. M. Greenlief, S. K. Kulkarni, and H. H. Sawin, *J. Vac. Sci. Technol.*, **A8**, 2965 (1990).
40. M. A. Mendicino and E. G. Seebauer, *Appl. Surf. Sci.*, **68**, 285 (1993).
41. P. Gupta, P. A. Coon, B. G. Koehler, and S. M. George, *Surf. Sci.*, **249**, 92 (1991).
42. R. P. Southwell and E. G. Seebauer, *Appl. Surf. Sci.*, In press.
43. E. G. Seebauer and C. E. Allen, *Prog. Surf. Sci.*, **49**, 265 (1995).
44. M. S. Chandrasekharaiyah, J. L. Margrave, and P. A. G. O'Hare, *J. Phys. Chem. Ref. Data*, **22**, 1459 (1993).

Nitrogen Doped Germania Glasses with Enhanced Optical and Mechanical Properties

T. Storgaard-Larsen

Brüel & Kjaer A/S, DK2850 Nærum, Denmark

C. V. Poulsen^a

Optoelectronics Research Centre, University of Southampton, Southampton SO17 1BJ, England

O. Leistiko

Microelectronics Centre, Technical University of Denmark, DK2800 Lyngby, Denmark

ABSTRACT

A new type of ultraviolet photosensitive germanium doped glass has been developed for use in the fabrication of optical waveguide structures. By adding ammonia to the source gases during a plasma enhanced chemical vapor deposition of these glasses, ultraviolet induced refractive index changes of up to 3.5×10^{-3} have been obtained. Although this is, to the best of our knowledge, a record for germanium doped silica films not photosensitized by hydrogen loading, our results show that even larger changes in the refractive index can be induced. Stable glasses with refractive indexes from 1.460 to 1.518 have been formed throughout the composition range from 0 to 30% germanium by including ammonia in the deposition process. Not only is it possible to increase the photosensitivity, but it is also possible to control stress in these films. Depending on the deposition and annealing conditions, these glass films can be made to exhibit a range of stress from compressive to low tensile when deposited on silicon wafers.

Because of its excellent optical properties, germanium doped glass is the most commonly used core material for low loss optical fibers. Interest in this material increased when it was shown by Hill *et al.*,¹ that it was photosensitive, i.e., that permanent changes of the refractive index could be made by irradiating this glass using ultraviolet (UV) light. The first UV written Bragg grating in an optical fiber was also made by Hill in 1978.¹ The final breakthrough, however, was first seen when Glenn *et al.*² demonstrated in 1988 that Bragg gratings could be written in optical fibers by exposing the side of the fiber to a two beam UV-light interference pattern. By varying the angle of incidence of the two beams, gratings having different periods could be made. The applications of photoinduced gratings include wavelength filters working as strain and

temperature sensors, dispersion compensating filters, and fiber laser mirrors. Despite great efforts, the mechanisms responsible for the photosensitivity of Ge-doped glasses is still not fully understood.

Recently, UV writing has also become a topic of great importance in thin film planar waveguide technology. Simplification of the process of planar waveguide fabrication, by direct UV laser writing of buried planar waveguide structures, including couplers, and splitters in three-layer SiO₂/GeO₂-SiO₂/SiO₂ glass films,^{3,4} could have a profound effect on the field of integrated optics. It should also be mentioned that the fabrication of planar waveguides employing photolithography and Ge-doped glasses also benefits from the use of UV writing techniques, in the realization of more advanced devices.

Only very few papers have been published on thin film processing of germanium doped glasses, however, in all

^a C.V.P. was a member of the research team at the Microelectronics Centre when this work was performed.

honesty it should be noted that integrated optical devices based on flame hydrolysis deposited germanium doped glasses are already commercially available from PIRI.⁵ Nourshargh⁶ reports on fabrication of germanium doped planar waveguides using microwave plasma chemical vapor deposition (MPCVD) and Rastani *et al.*⁷ report on low pressure chemical vapor deposition (LPCVD) of germanium doped oxides.

Both UV written³ and more typical buried planar waveguides based on plasma enhanced chemical vapor deposition (PECVD) Ge-doped glass have been demonstrated.^{8,9} Also, other groups have begun reporting on activities in thin film processing of PECVD germanium doped glasses.¹⁰

Special Requirements for an Opto-Mechanical Sensor

For this work the interest was in making an opto-mechanical accelerometer based on strain sensing by a UV light written Bragg grating in a planar waveguide bridge.¹¹ To achieve a nondistorted mechanical frequency response and a high mechanical sensitivity it was necessary that the bridges, which were 1 mm in length, had a low tensile stress and small cross-sectional dimensions. Thus, a new type of germanium doped glass had to be developed. In order to enable fabrication of a functional device based on the cladding glass described in the article by Storgaard-Larsen *et al.*,¹¹ our germanium doped glass had to fulfill the following requirements: (i) high refractive index, >1.50 . The cladding glass (SiON100) reported in the previous paper,¹² that seemed to be the best choice for our waveguide bridges, had a refractive index of 1.477. In order to achieve low tensile stress without signs of cracking, the total thickness of the waveguide layer should not exceed 5 to 6 μm . For the wave to be well guided, at these, relative to the optical wavelength (1.55 μm), small waveguide dimensions, a large index change (0.02 to 0.05) between core and cladding is needed;¹³ (ii) low tensile stress: a core glass having high compressive stress would necessarily require a cladding glass having an even higher tensile stress, in order to achieve the required total stress, i.e., thermal stress + intrinsic stress, of the waveguide structure. Also, a nonuniform stress distribution in the cross section of the waveguide layer can cause unwanted birefringence. Earlier work has shown that the maximum stress (tensile) is obtained by annealing the glasses at approximately 800°C;¹² (iii) photosensitive; index modulation better than 5×10^{-4} should be achievable; to fabricate the Bragg grating specified in the paper by Storgaard-Larsen *et al.*,¹¹ an index change in the order of 2×10^{-3} is desired.

The typical index range that can be obtained with germanium doped oxide is between 1.46 (SiO_2) and 1.61 (GeO_2).⁷ However, our first requirement cannot be fulfilled with any known types of germanium doped glasses. Germanium doped glasses are known to be hydroscopic. At GeO_2 concentrations exceeding 20%, films annealed at temperatures around 800°C start becoming unstable, and tend to become water soluble.^{7,8} Hence, the upper limit of the index range that can be covered by germanium doping of high quality silica glasses is limited to about 1.48 to 1.49.

It is well known that slightly higher refractive indexes can be achieved in optical fibers by applying processing temperatures as high as 2000°C.¹⁴ Refractive indexes in the range of 1.50 are obtained at germanium concentrations of 25%.

According to Miller *et al.*,¹⁴ the thermal expansion coefficient of germanium doped glass increases linearly with the Ge concentration. At a germanium to silicon ratio of about 25%, a match to silicon is achieved (2.6 ppm). By matching the coefficients of thermal expansion of germanium doped glass to that of silicon, it is possible to eliminate the effects of thermal stress and, thus, the achievement of tensile stress in the glass will depend only on the intrinsic stress.¹²

In this paper we describe the development of a new type of PECVD germanium doped glass capable of fulfilling our special requirements.

Experimental

A load locked parallel-plate STS (E-type) PECVD reactor was used for deposition of the glasses in this work. The reactor can be driven both by a low frequency (380 kHz) RF power supply and a high frequency (13.56 MHz) RF power supply. The reactor contains two parallel 10 in. diameter electrodes separated by a distance of 22 mm. The lower electrode, which supports the substrate, is grounded. A schematic of the PECVD reactor is shown in Fig. 1. A more detailed description of the PECVD reactor can be found in the thesis by Mattsson.¹⁵

Annealing was carried out in a Tempress furnace at temperatures ranging from 700 to 1100°C in a N_2 atmosphere. To avoid thermal shocks, slow loading/unloading (10 mm/min) was applied and dummy wafers were used in both ends of the quartz furnace boat. Warm-up, from the standby temperature of 700°C, was done at a speed of 10 K/min while cooling was done at 4 K/min. Also, argon was tested as the ambient atmosphere, but no significant changes in film stresses and refractive indexes were measured when using this more expensive alternative.

The total mechanical stress of the films at room temperature was determined with a Tencor surface profiler by measuring the curvature of the silicon wafer before and after the deposition and after each of the following thermal annealing steps. For stress measurements, film thicknesses of more than 2 μm were preferred to ensure high accuracy. The reproducibility of the stress measurements were within ± 1 MPa. Finally, the applied sign convention is positive (+) when tensile stress and (−) when compressive. The measured stress (σ_t) can be written as the sum of the intrinsic stress (σ_i) related to deposition kinetics and the thermal stress (σ_{th}) attributed to difference of thermal expansion coefficients of film and the silicon substrate.¹²

The thickness and refractive index were measured with a prism coupler system¹⁵ capable of measuring the refractive indexes up to 1.52 with an accuracy better than $\pm 2 \times 10^{-4}$ and determining the thickness with an accuracy of ± 0.02 μm . The system which is operated at an optical wavelength of 632.8 nm is used on glass films thicker than 2 μm . Each film was measured at the center of the wafer, and in radial distances of 1 and 2.5 cm from the center. Four in. diam, 450 to 550 μm thickness, single-side polished (100) silicon wafers were used as substrates during development of the PECVD glasses.

As mentioned earlier, standard low frequency PECVD germanium doped glasses become unstable at high germanium concentrations (>20 to 25%) indicating porosity and water solubility.^{7,8} Since high germanium concentrations would be needed in order to fulfill our special requirement for a high refractive index ($n > 1.50$), a new type of glass had to be developed for this project. In the previous paper,¹² the effect of nitrogen doping on high frequency (13.56 MHz) PECVD SiO_2 films was discussed. The silicon oxynitride films offered high refractive indexes and stresses (tensile), and low etch rates. Inspired by these interesting glass properties the attempt of developing a silicon/germanium oxynitride ($\text{SiO}_x\text{N}_y\text{H}_z - \text{GeO}_x\text{N}_y\text{H}_z$) was initiated by adding ammonia to the gas mixture. The resulting process-

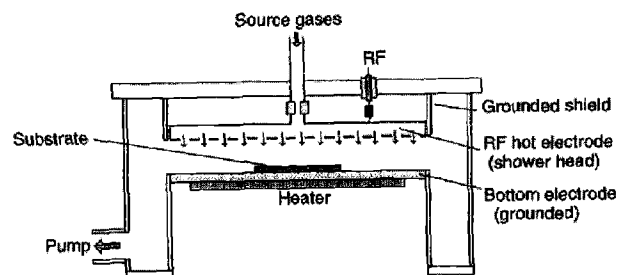


Fig. 1. Schematic of the parallel plate PECVD reactor.¹⁵

Table I. Processing conditions.

Ge-doped glass		Process conditions
Flow, sccm	SiH ₄	12 to 17
	GeH ₄	0 to 5
	(SiH ₄ + GeH ₄)	17
	N ₂	833
	N ₂ O	1600
	NH ₃	0 to 400
RF-power, W	lf 380 kHz	380
Pressure, mTorr		400
Temperature, °C		300

ing conditions for the glasses are shown in Table I. Again, as for the processing conditions for silicon oxynitride given in our previous paper,¹² the presence of N₂ in the gas mixture results from changing from diluted to undiluted silane. The total flow of silane plus germane was kept constant at 17 sccm, in order to focus on effects related to changes in the germane to silane gas composition ratio. It should be mentioned that the adding of ammonia to the gas mixture lowers the partial pressures of the other gases due to an increase in the total gas flow.

Results and Discussion

Figure 2 shows the variation of the refractive index of nitrogen doped glasses annealed at 800°C, as a function of the mole fraction of germane in the silane/germane gas mixture, which is kept at a total of 17 sccm. The ammonia flow is varied from 0 to 400 sccm. Apart from a few exceptions, the refractive index is seen to increase almost linearly with the mole fraction of germane. The sudden divergence from linearity at increasing germane mole fractions for 0 sccm NH₃ flow, is due to the increase in porosity. Annealing the same glasses for 2 h at 1100°C (dashed curve), leads to a densification of the glasses, "re-establishing" a linear dependence between the refractive index and the molar concentration of germane. The intersection of the ordinate at a refractive index of 1.46 for ammonia flows in the range from 0 to 200 sccm, indicates that the nitrogen is only bonded to germanium. However, this is contradicted by the results of the films having higher ammonia flows. It is also interesting to note a nonlinear dependence of the refractive index on ammonia gas flow is seen when no GeH₄ is added to the gas mixture. Finally, we call attention to the fact that a glass with a measured

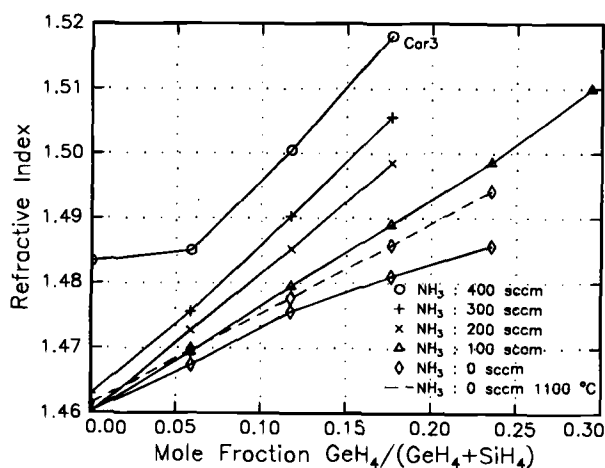


Fig. 2. The refractive index as a function of germane mole fraction at varying ammonia flows. Solid curves: annealing: 2 h at 800°C; No. S90 - S95, No. S102 - S105, No. TU34-TU37, No. S157, No. S160, No. S162 - S168. Dashed curve: annealing: 2 h at 800°C + 2 h at 1100°C, No. S157, S162 - S165.

refractive index of 1.518 was obtained at germania and ammonia gas flows of 3 and 400 sccm, respectively.¹²

Figure 3 shows the refractive index vs. the ammonia flow for germane gas flows of 2 and 3 sccm. It appears that the refractive index depends more or less linearly on the ammonia flow for these processing conditions. Furthermore, the differences in gradients for the two curves supports the conclusion that the amount of nitrogen incorporated in the film depends on the content of germane in the gas mixture.

Figure 4 illustrates the total stress, as-deposited, and after 2 h of annealing, as a function of the germane for ammonia gas flows of 100 and 200 sccm. The stress is seen to increase with the content of GeH₄ in the gas flow. This supports the assumption that the contribution from thermal stress is reduced when germanium is incorporated in the glass.

The total stress as a function of ammonia flow for germane flows of 2 and 3 sccm is shown in Fig. 5. The total stress is seen to decrease almost linearly with the ammonia flow. Upon annealing at 800°C, the influence of ammonia doping on the total stress becomes linear. The deviation from almost linear behavior of the curve representing the 3 sccm GeH₄ film supports our conclusion that some of the films become porous if no ammonia is added to the gas mixture.

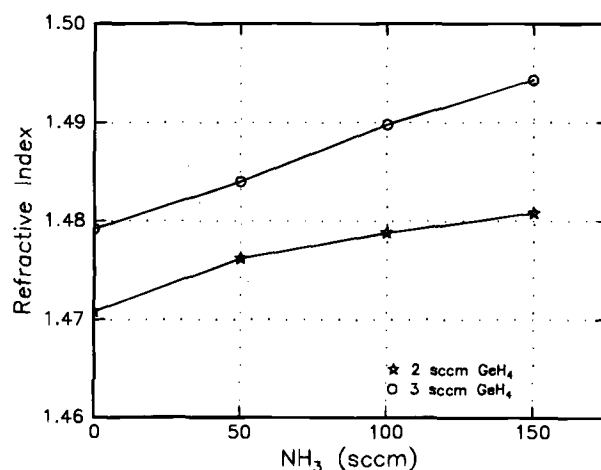


Fig. 3. The refractive index vs. ammonia flow at germane flows of 2 and 3 sccm (= germane mole fractions of 12 and 18%). Annealing: 2 h at 800°C; No. S80 - S83, No. S85 - S88.

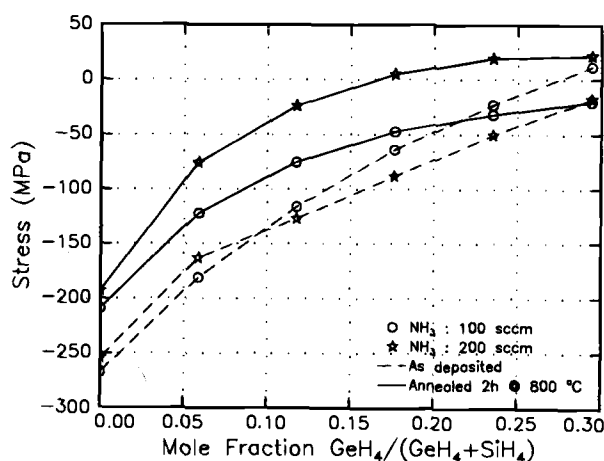


Fig. 4. The total stress as a function of germane mole fraction at ammonia flows of 100 and 200 sccm. Dashed curves: as-deposited, No. S90 - S95, No. S102 - S107. Solid curves: annealing: 2 h at 800°C; No. S90 - S95, No. S102 - S107.

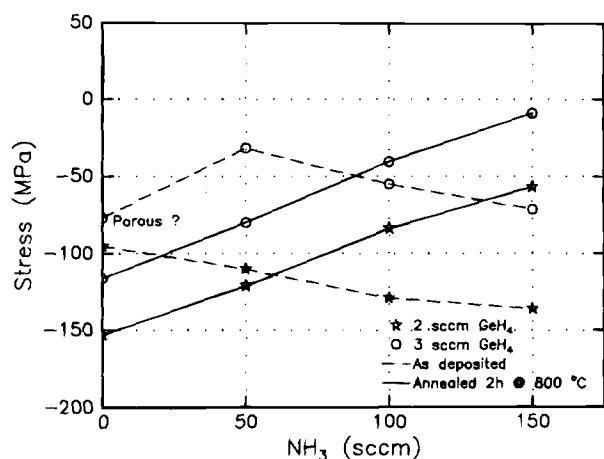


Fig. 5. The total stress vs. ammonia flow at germane flows of 2 and 3 sccm (= germane mole fractions of 12 and 18%). Dashed curves: as-deposited, No. S90 - S95, No. S102 - S107. Solid curves: annealing: 2 h at 800°C; No. S90 - S95, No. S102 - S107.

The potential of fabrication of films having a zero total stress, as-deposited, is clearly demonstrated with the results shown in the Fig. 4 and Fig. 5. Furthermore, the low stress levels, as-deposited, can be maintained after 2 h of annealing at 800°C. These observations can be of major interest for so-called surface micromachining, where a low stress sacrificial layer between substrate and intended mechanical elements can be crucial.

The influence of the ammonia gas flow on the BHF etch-rate of the films is shown in Fig. 6. Even small ammonia gas flows, of about 50 sccm, can change germanium doped films from presumably being porous, after 2 h of annealing at 800°C, into films exhibiting etch rates below the level of thermally grown oxides (750 Å/min). The etch rates are seen to saturate at ammonia flows exceeding 100 sccm. At this level of ammonia flow, the BHF etch rate is seen to decrease with increasing germane gas flow ratio in the range that has been investigated (0 to 30%). Nearly identical etch rates are achieved by annealing the films 2 h at 1100°C in a N₂ atmosphere (see dashed curve), instead of adding ammonia to the gas mixture.

When annealing nitrogen doped films at 1100°C, localized microscopic blistering effects were seen. At high ammonia levels, the blisters turned into circular holes and a deposition of material onto the neighboring wafer on the

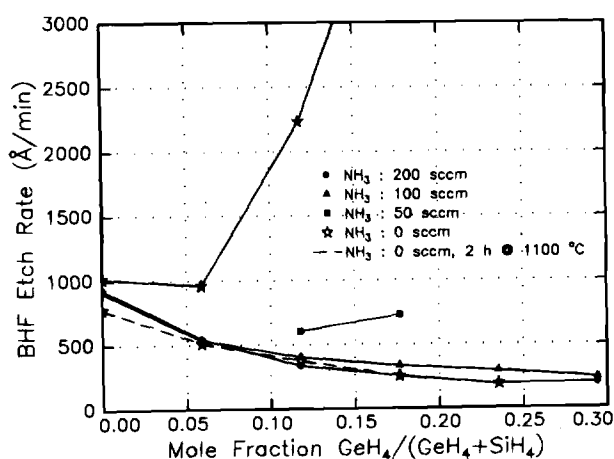


Fig. 6. BHF etch rate as a function of germane mole fraction at varying ammonia flows. Solid curves: annealing: 2 h at 800°C; No. S81, No. S86, No. S90 - S95, No. S102 - S107, No. S162 - S167. Dashed curve: annealing: 2 h at 1100°C; No. S162 - S167.

quartz boat (spacing 5 mm), could be seen. Kern *et al.*¹⁶ have observed similar phenomena on PECVD silicon nitride films upon annealing. The blistering was explained as being stress relief of films under compression and the plastic deformation is believed to be caused by outgassing of dissolved hydrogen.

At germane mole fractions exceeding about 10%, experiments with BHF etching showed indications of inhomogeneities in the glasses. Ten minutes of BHF etching resulted in a coarse surface morphology which appeared white due to diffuse scattering of white light. The roughness was seen to increase with the germanium concentration. However, addition of ammonia to the gas mixture was found to improve the glass quality significantly. The amount necessary to prevent the films from appearing white after BHF etching increased with the germane gas flow. The low etch rates (200 to 300 Å/min) imply that the roughness of the surface morphology on the etched films is not due to porosity. Furthermore, annealing at 1100°C (NH₃: 0 sccm) did not reduce the problem.

Deposition rate.—The deposition rate was seen to increase with germane mole fraction, typically this ranges from 1200 to 1600 Å/min.

Uniformity.—The uniformity of the glass thickness was seen to decrease with increasing amount of glass previously deposited on to the walls and electrodes of the deposition chamber. Thickness uniformity on a wafer ranged from 1 to 4%, being best after a physical cleaning of the deposition chamber. The variations in refractive index across a wafer were within the uncertainty of the prism coupler system ($\pm 2 \times 10^{-4}$).

Reproducibility.—The condition of the chamber did not seem to affect the refractive index significantly. Refractive indexes could be reproduced better than 0.001 if no major changes were made to the system, such as replacement of certain parts of the PECVD system. The condition of the chamber was monitored by deposition and characterization of test wafers.

Photosensitivity

The refractive index of germania doped glasses can be increased through absorption of visible or UV light.¹⁷⁻¹⁹ The relative index change is believed to be due to a redistribution of defects within the glass. Typically, the UV induced refractive indexes are categorized in two types.²⁰ Type I is formed at low light intensities, type II, however, is formed at high light intensities, *e.g.*, from a UV excimer laser, sometimes causing visible deformations of the glass. Type II index changes are thermally stable up to 800°C while type I begins to disappear at temperatures of about 300°C.

Despite considerable research effort, the mechanisms responsible for the photosensitivity are not fully understood. It has been shown,¹⁷ that the UV photosensitivity depends to a large extent on the germanium concentration. The fact, that the glass quality becomes questionable at germanium concentrations exceeding 20 to 25%, puts a constraint on the achievable photosensitivity. Typically, index changes in the order of 10^{-5} to 10^{-4} can be formed in standard germania doped optical fibers.

Different techniques to further enhance photosensitivity by deliberately generating defects in the glass have been demonstrated.^{17,18} By controlling the fabrication process, the concentration of the oxygen deficient germania defects (GeO) can be increased, leading to an improvement of the photosensitivity. Hydrogen (H₂) loading of germania doped glasses, in high pressures (200 bar) or at elevated temperatures, has been used to achieve index changes as high as 0.011.¹⁸ However, the long-term stability of refractive index changes formed by this technique is not acceptable, and transmission losses in the IR region of the waveguides increase significantly due to formation of hydroxyl groups (OH) having a peak absorption at a wavelength of 1380 nm. The broad OH absorption band also creates increased losses at 1.55 μm. Replacing hydrogen with the

more expensive deuterium (D_2) is believed to reduce the formation of OH. Finally, boron codoping of germania doped films has been used to enhance photosensitivity. It is suggested that boron promotes a stress relaxation effect in the glass.

For direct UV-writing of planar waveguides, the refractive index change should preferably be 5×10^{-3} or higher.⁴ This is in contrast to writing of Bragg gratings where 5×10^{-4} is sufficient.

Measured UV induced index changes up to 2.5×10^{-3} have previously been reported for hydrogen loaded PECVD germania doped oxides.³ Combining hydrogen loading and boron codoping, films formed by flame hydrolysis have exhibited index changes calculated to be 7.5×10^{-3} .

The silicon/germanium oxynitride films described in this paper obviously fulfilled our special requirements for high refractive indexes and tensile stresses. However the question remains: "How does nitrogen codoping, by adding ammonia to the gas mixture, affect the photosensitivity of germania doped PECVD glasses?"

Exposure of films to UV light from a 193 nm excimer laser resulted in surprisingly high index changes, which could be measured with the prism coupler system. Type A films and type B films, both processed with a NH_3 flow of 400 sccm and annealed at 800°C, and both having refractive indexes of about 1.495, were compared. The type A film was processed from the recipe shown in Table I, while the recipe of the type B film differs from this in that the RF power used was 800 W and the pressure was 600 mTorr. The germane gas flows of the two films were 2 and 4 sccm, respectively. Table II shows the process conditions for the two films as well as the measured refractive index changes Δn , achieved after UV exposures of 16 min which was equivalent to a total fluence of 4800 J/cm². The pulse energy was about 100 mJ/pulse at a pulse duration of 20 ns at 20 pulses/s, and the spot size was around 2×20 mm, giving an intensity of around 12 MW/cm² at the surface of the glass film. Also, lower fluences were applied on the same wafer indicating that saturation does not occur at 4800 J/cm².

For a nonhydrogen loaded germania doped film the photoinduced index change of 3.5×10^{-3} exhibited by the type A films must be considered very high. The type B film shows a lower index change despite a two times higher germane concentration in the gas phase.

It is known that the presence of ammonia in the gas mixture enhances the incorporation of hydrogen in ordinary PECVD silicon nitrides and oxynitrides. We might explain the photosensitivity by a high content of hydrogen due to the presence of ammonia in the gas mixture. In the hydrogen loading process, the physically dissolved hydrogen (H_2) first reacts with the glass during UV exposure and thereby forms defects in the glass. Since the exposure of our films to UV light takes place after an 800°C anneal in N_2 we conclude that the H_2 is more tightly bonded to the glass matrix than is the case with hydrogen doping.

An alternative hypothesis to explain the enhanced photosensitivity could be based on the presence of nitrogen in the films. Nitrogen alters the glass matrix, creating more absorption bands which might result in a higher degree of absorption of the UV photons again leading to a higher photosensitivity.

Table II. Process conditions for the two films, A and B, along with the measured refractive index changes Δn achieved after UV light exposures having a total fluence of 4800 J/cm².

Glass type:	Type A	Type B
$GeH_4/(GeH_4 + SiH_4)$	$\approx 12\%$	$\approx 24\%$
NH_3 flow, sccm	400	400
RF- power, W	380	800
Pressure, mTorr	400	600
UV induced Δn	$>3.5 \times 10^{-3}$	$>1.8 \times 10^{-3}$

UV written multimode waveguides in three-layer glass film structures based on the type A glass, has shown propagation losses as low as 0.3 dB/cm.²¹

Conclusions

Addition of ammonia (NH_3) to a $GeH_4-SiH_4-N_2-N_2O$ gas mixture in a PECVD reactor produced a new kind of silicon/germanium oxynitride glass.

The refractive index was seen to linearly depend on germane mole fraction ($GeH_4/(SiH_4 + GeH_4)$) and ammonia flow. While typical Ge-doped glasses can have refractive indexes up to about 1.50, without being water soluble, this new type of glass offers low loss, nonporous, low etch rate films having refractive indexes up to about 1.52. Adding ammonia to the gas mixture was seen to change films, which are presumably porous, into dense films exhibiting BHF etch rates below the level of thermally grown oxide, which are more typical of $SiON$ or Si_3N_4 . Also the roughness of the glass surface after etching in BHF was seen to improve with the ammonia gas flow.

The total stress of films annealed at 800°C was seen to increase with the germane mole fraction and the ammonia flow. As-deposited films which were stress-free or having low tensile stress were demonstrated. Annealing these films at 800°C only caused modest changes of the total stress. This glass might be a candidate as a sacrificial layer in surface micromachining.

UV-radiation of type A glass at a wavelength of 193 nm at room temperature produces permanent changes in the refractive index in excess of 3.5×10^{-3} . To our knowledge, this is the highest UV-induced index change ever reported on a Ge-doped glass film which has not been hydrogen loaded.

Manuscript submitted Aug. 13, 1996; revised manuscript received March 25, 1997.

Brüel & Kjaer A/S assisted in meeting the publication costs of this article.

REFERENCES

1. K. O. Hill, Y. Fujii, D. C. Johnson, and B. Kawasaki, *Appl. Phys. Lett.*, **32**, 647 (1978).
2. W. H. Glenn, G. Meltz, and E. Snitzer, U.S. Pat. 4,725,110 (1988).
3. M. Svalgaard, C. V. Poulsen, A. Bjarklev, and O. Poulsen, *Electron. Lett.*, **30**, 1401 (1994).
4. G. D. Maxwell and B. J. Ainslie, *ibid.*, **31**, 95 (1995).
5. Photonics Integration Research Inc., Sales brochure on planar waveguides (1993).
6. N. Nourshargh, E. M. Starr, and T. M. Ong, *Electron. Lett.*, **25**, 981 (1989).
7. S. Rastani and A. Reisman, *This Journal*, **137**, 1288 (1990).
8. J. O. Gulløv, M.S. Thesis, Mikroelektronik Centret, The Technical University of Denmark (1995).
9. B. Rose, M.S. Thesis, Mikroelektronik Centret, The Technical University of Denmark (1995).
10. M. V. Bazylev, M. Gross, P. L. Chu, and D. Moss, in *Photosensitivity and Quadratic Nonlinearity in Glass Waveguides, Fundamentals and Applications*, Vol. 22, p. 108, OSA, Portland, OR (1995).
11. T. Storgaard-Larsen, S. Bouwstra, and O. Leistiko, *Sens. Actuators*, **A52**, 25 (1996).
12. T. Storgaard-Larsen and O. Leistiko, *This Journal*, **144**, 1505 (1997).
13. B. E. A. Saleh and M. C. Teich, *Fundamentals of Photonics*, John Wiley & Sons, Inc., New York (1991).
14. *Optical Fiber Telecommunications*, S. E. Miller and A. G. Chynoweth, Editors, Academic Press, New York (1979).
15. K. E. Mattsson, Ph.D. Thesis, The Technical University of Denmark (1994).
16. W. Kern and R. S. Rosler, *J. Vac. Sci. Technol.*, **14**, 1082 (1977).
17. R. J. Campbell and R. Kashyap, *Int. J. Optoelectron.*, **9**, 33 (1994).
18. D. L. Williams, B. J. Ainslie, R. Kashyap, G. D. Maxwell, J. R. Armitage, R. J. Campbell, and R. Wyatt, *Proc. SPIE*, **2044**, 55 (1993).

19. P. J. Lemaire and T. Erdogan, in *Photosensitivity and Quadratic Nonlinearity in Glass Waveguides, Fundamentals and Applications*, Vol. 22, p. 78, OSA, Portland, OR (1995).
20. P. St. J. Russell, J.-L. Archambault, and L. Reekie, *Physics World*, pp. 41-46 (Oct. 1993).
21. C. V. Poulsen, T. Storgaard-Larsen, J. Hübner, and O. Leistiko, *Electron. Lett.*, Submitted.

Deposition of Carbon-Rich Film during Etching of Aluminum and Aluminum Oxide Surfaces

J. Tonotani, S. Saito, and E. Nishimura

Toshiba Corporation, Manufacturing Engineering Research Center, 33 Shin-Isogo-cho, Isogo-ku, Yokohama 235, Japan

ABSTRACT

The deposition of carbon-rich film during etching of aluminum and aluminum oxide surface is studied. When the etching is carried out using a $\text{BCl}_3/\text{CH}_3\text{OH}$ plasma excited in a parallel-plate magnetron-reactive ion etching reactor, deposits are observed on both aluminum and aluminum oxide surfaces. Analyses of the etched surfaces by x-ray photoelectron spectroscopy and Fourier transform infrared spectroscopy show that the deposits consist mainly of carbon with C-C bonds. The analyses also suggest that the deposit is accumulated more easily on the aluminum surface than on the aluminum oxide surface when a small amount of CH_3OH is added to BCl_3 . We consider that this difference in the deposition characteristics is dependent on the oxidation rate of the deposits due to the existence of oxygen on the etched surface. When we selectively etch aluminum oxide against aluminum as an application of these deposition phenomena, a good etching selectivity of more than ten is obtained.

Introduction

Due to the increase in the size of thin film transistor liquid crystal displays (TFT-LCDs) and in the number of pixels they contain, it has become necessary to use aluminum gate lines to overcome the problem of drive pulse delay.¹⁻³ Aluminum, however, is difficult to handle because of its chemical and thermal instability; it can be eroded by acid or alkali and it can diffuse into an adjacent layer during heating.⁴ Therefore, when aluminum gate lines or signal lines are used in TFT-LCDs, they should be covered by an aluminum oxide layer to protect them from chemical and thermal damage.⁵ In order to pattern the double-layer gate lines by dry etching, the etching characteristics of both aluminum and aluminum oxide should be known in detail. Usually, in the fabrication of very large scale integrated (VLSI) circuits, gas containing chlorine is used in aluminum dry etching^{6,7} because aluminum reacts very easily with chlorine and the products AlCl_3 and Al_2Cl_6 have high vapor pressures. However, this high reactivity of aluminum with chlorine often makes the etching process difficult. This is why polymer-generating species such as CHF_3 and CH_3Cl are added to gas containing chlorine when an anisotropic or tapered profile of etched aluminum is required.⁷ It has been reported that deposits which protect aluminum sidewalls from chlorine attack consist mainly of carbon and chlorine.⁷ However, the exact structures and deposition mechanisms of such polymers are not yet well understood. Only a few studies on the etching mechanism of aluminum oxide have been made.⁸

In this work, the deposit produced on aluminum and aluminum oxide surfaces when $\text{BCl}_3/\text{CH}_3\text{OH}$ gas mixture is used as the etching gas is investigated. Because of the difficulty of analyzing the sidewalls, only the front surfaces, which were exposed to ion bombardment, are analyzed by x-ray photoelectron spectroscopy (XPS) and Fourier transform infrared spectroscopy (FTIR). The surface analyses of both aluminum and aluminum oxide and optical emission spectroscopy of $\text{BCl}_3/\text{CH}_3\text{OH}$ plasma have led to a better understanding of the structure of the deposit and the deposition mechanism. Finally, we try to apply the deposition phenomenon to selective etching of aluminum oxide against aluminum.

Experimental

Test samples were prepared using 6 in. silicon wafers with 100 nm thick thermal silicon oxide layers. An alu-

minum film 350 or 400 nm thick was deposited by magnetron sputtering (MCH-9000; ULVAC). Aluminum oxide samples were produced by anodic oxidation of the aluminum top surface to form 100 nm thick aluminum oxide layer. In anodic oxidation,^{9,10} an aqueous solution of a mixture of ammonium tartrate and ethylene glycol was used as the electrolyte,^{5,9,10} and the current density between the platinum cathode and aluminum anode was kept at about 1 mA/cm^2 . The etching reactor shown in Fig. 1 is of a magnetron-reactive ion etching (RIE) type, where the magnetic field has a strength of about 200 G immediately beneath the magnet and about 50 G immediately above the electrode to which a radio frequency (RF) is applied. The wafer was cut into 3×3 cm pieces, and $\text{BCl}_3/\text{CH}_3\text{OH}$ gas mixture was used as the etching gas. In this study, only the gas flow rate ratio of $\text{BCl}_3/\text{CH}_3\text{OH}$ was varied. The process pressure, the applied RF (13.56 MHz) power and the powered electrode temperature were kept constant at 2.0 Pa, 200 W (corresponding power/electrode area ratio is 1.5 W/cm^2) and 20°C, respectively. The etched depth was measured using a step measurement tool (Dektak; Veeco

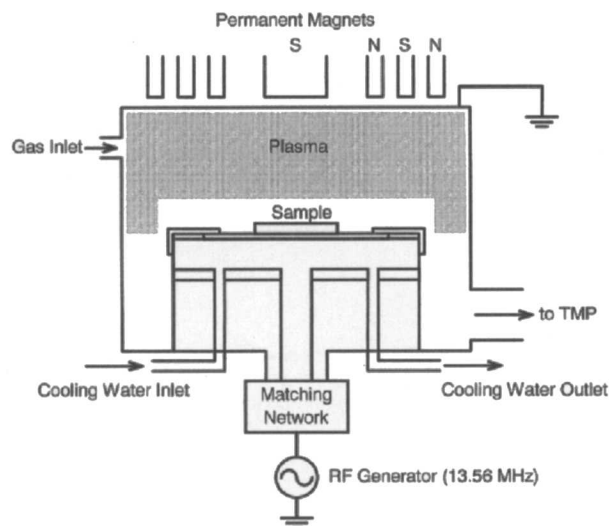


Fig. 1. Schematic diagram of etching reactor.